

UKAEA-CCFE-PR(22)52

R. Scannell, J. G. Clark, Y. Kim, D. Kos, M. Maslov, L.  
Giudicotti

# **Polarimetric Thomson scattering measurements in 1 JET high Temperature Plasmas**

Enquiries about copyright and reproduction should in the first instance be addressed to the UKAEA Publications Officer, Culham Science Centre, Building K1/O/83 Abingdon, Oxfordshire, OX14 3DB, UK. The United Kingdom Atomic Energy Authority is the copyright holder.

The contents of this document and all other UKAEA Preprints, Reports and Conference Papers are available to view online free at [scientific-publications.ukaea.uk/](https://scientific-publications.ukaea.uk/)

# **Polarimetric Thomson scattering measurements in 1 JET high Temperature Plasmas**

R. Scannell, J. G. Clark, Y. Kim, D. Kos, M. Maslov, L. Giudicotti



# 1 Polarimetric Thomson scattering measurements in 2 JET high Temperature Plasmas

---

3 **R. Scannell<sup>a,c</sup>, J. G. Clark<sup>a,b</sup>, Y. Kim<sup>a</sup>, D. Kos<sup>a</sup>, M. Maslov<sup>a</sup>, L. Giudicotti<sup>c</sup> and JET**  
4 **Contributors\***

5 <sup>a</sup>*UKAEA/CCFE, Culham Science Centre, Abingdon, Oxon OX14 3DB, United Kingdom*

6 <sup>b</sup>*Department of Electrical Engineering and Electronics, University of Liverpool, Liverpool, L69 3GL*

7 <sup>c</sup>*Department of Physics and Astronomy, Padova University, Via Marzolo 8, 35131 Padova, Italy*

8 <sup>d</sup>*E-mail: [rory.scannell@ukaea.uk](mailto:rory.scannell@ukaea.uk)*

9 \* See the author list of Overview of the JET preparation for Deuterium-Tritium Operation by E Joffrin et  
10 al 2019 Nucl. Fusion 59 112021 <https://iopscience.iop.org/article/10.1088/1741-4326/ab2276>

11 **ABSTRACT:** Thomson scattered light is polarised in the same orientation as the incident laser  
12 beam at low electron temperatures ( $T_e$ ). At high  $T_e$  part of the spectrum begins to become  
13 randomly polarised due to relativistic reasons. First measurements of the depolarised Thomson  
14 scattering spectrum during were obtained from JET pulses in 2016. This paper builds upon these  
15 initial measurements with new measurements obtained during 2021. These new measurements  
16 improve upon first results, in particular by obtaining spectral measurements of the depolarised  
17 spectrum. The recent JET campaign was well suited to these measurements with long and hot  
18 plasmas. The resulting data are averaged over many plasmas and laser pulses to obtain a  
19 measurement of the amount of ‘p’ and ‘s’ scattered light as a function of  $T_e$ . This experimentally  
20 obtained ‘p/s’ ratio versus  $T_e$  is then fitted and found to show reasonable agreement with the  
21 theoretically predicted depolarised fraction. Error estimates on the measured ‘p/s’ have been  
22 obtained and show that the measurements are meaningful. This is good news for ITER for  
23 which the intention is to use this measurement as a check on the  $T_e$  determined by the core  
24 plasma Thomson scattering diagnostic by conventional spectral measurement techniques.

25 **KEYWORDS:** Polarimetric, Thomson scattering, laser diagnostics

---

26	<b>Contents</b>	
27	<b>1. Introduction</b>	<b>1</b>
28	<b>2. Installation on JET</b>	<b>2</b>
29	<b>3. Overview of Dataset</b>	<b>3</b>
30	<b>4. Polarimetric Measurements</b>	<b>4</b>
31	<b>5. Conclusions</b>	<b>5</b>
32		
33		
34		
35		

---

## 36 1. Introduction

37 The ITER Core Plasma Thomson Scattering (CPTS) diagnostic is required to measure up  
38 to 40keV. This implies measuring down to wavelengths of  $\sim 400\text{nm}$  using conventional or  
39 ‘spectral’ Thomson scattering (Scannell R. et al 2017) from a 1064nm laser. This low  
40 wavelength requirement arises due to the broad spectral width at  $T_e=40\text{keV}$  at the large CPTS  
41 scattering angles of  $\sim 160\text{degrees}$  in the core. Measuring at low wavelengths is challenging as  
42 many of the expected losses due to neutron or radiation damage of optics or fibres will be  
43 largest in lower wavelength region (400-700nm). Similarly, line emission will be largest in this  
44 same wavelength region.

45 Polarimetric Thomson scattering is an alternative Thomson scattering technique, not  
46 currently deployed on existing machines. It takes advantage of the fact that a small fraction of  
47 the Thomson scattering spectrum becomes depolarised at high electron temperature ( $T_e$ ). The  
48 depolarisation increases with  $T_e$  for a given scattering angle and is uniform across the spectrum.  
49 These properties mean that an increase in the lower wavelength limit, due to losses or line  
50 emission, would not impact the ability to infer  $T_e$  from polarimetric measurements. In fact,  
51 polarimetric measurements would be immune to any potential unquantified systematics in  
52 spectral transmission, provided the spectral transmission is not polarisation dependent.

53 The technique of polarimetric Thomson scattering was first proposed in (Orsitto F et al  
54 1999). Since then, there have been significant advances in the theoretical basis (Segre S.E. et al  
55 2000)(Parke E. et al 2014)(Mirnov V.V. et al 2016) The amount of depolarisation may now be  
56 readily determined for a given  $T_e$  and scattering angle. In a spectral Thomson scattering system,  
57 the injected light is typically orthogonal or ‘s’ polarised (senkrecht – perpendicular) with respect  
58 to the scattering plane formed by incident and scattering vectors. Depolarised light is randomly  
59 polarised and therefore equal in both ‘s’ and ‘p’ (parallel) polarisations. In a spectral Thomson  
60 scattering system, ‘p’ polarised light is often removed by polarisers as it is considered to contain  
61 no scattered light. For a polarimetric Thomson scattering system, the ‘s’ and ‘p’ components of  
62 the scattered light are separately measured and quantified and the ratio of the two (‘p/s’) used to  
63 infer  $T_e$ .

---

64 At a 90 degree scattering angle, the fraction of light in the non-standard ‘p’ polarisation  
65 increases approximately linearly at 0.191%/keV as calculated from theoretical predictions in the  
66 range 1-10keV. The JET data that are considered in this paper are taken at a scattering angle  
67 91.4 degrees and up to temperatures of ~9keV from the HRTS (high resolution Thomson  
68 scattering) diagnostic. Hence for these scattering events a p/s ratio of up to ~1.53% is expected  
69 at  $T_e=8\text{keV}$ . The ITER CPTS diagnostic operates from ~131 degrees at the low field side edge,  
70  $r/a\sim 0.85$ , to ~160 degrees at the plasma center. The depolarisation is significantly less at a 160  
71 degree scattering angle such that the JET results at 6keV are approximately equivalent to ITER  
72 results at 20keV. This is illustrated in figure 1 which shows the relative sensitivity at these two  
73 scattering angles. The CPTS system will allow for more averaging than JET as it is based on a  
74 100Hz rather than a 20Hz laser and with longer plasma pulse durations. Additionally, the ITER  
75 system can provide polarimetric measurements over all spatial points observed compared to at  
76 just one point for JET.

77  
78

## 79 2. Installation on JET

80 The first polarimetric Thomson scattering measurement on a fusion machine were obtained  
81 on JET during the DD campaign in 2016, from pulses 92038-92504 (Giudicotti et al, 2018). We  
82 will refer to these measurements as DD in contrast to our recent measurements during DT. This  
83 campaign was the second Deuterium Tritium campaign on JET (DTE2), since the initial DT  
84 campaign in 1997, and as such had a goal to maximise fusion energy produced. This led to long  
85 high temperature plasmas which were particularly suitable for the polarimetric measurements.  
86 From the initial results during DD the ratio of ‘p’ to ‘s’ light was obtained as function of  $T_e$  by  
87 taking each pulse and averaging the scattered signals from that JET pulse during the heating  
88 phase. These results indicated that polarimetric Thomson scattering works as a technique and is  
89 in line with theoretical predictions.

90 The motivation for new measurements during the DT campaign are as follows:

- 91 • Significant variation in the p/s ratio was observed in the DD measurements. This is  
92 inherent from the fact that the number of ‘p’ scattered photons is very low and  
93 motivates further measurements to confirm the initial result. Estimating the uncertainty  
94 on the determined  $d(p/s)/dT_e$  in these new measurements was another key goal.
- 95 • After the initial measurements during DD a Raman calibration was performed. The  
96 result of this calibration implied a significant difference in the sensitivity of the fibre  
97 with the ‘p’ polarizer versus that of the fibre with the standard ‘s’ polarizer. This arose  
98 from the fact that the ‘s’ fibre was misaligned to the laser beam making it ~6.7 times  
99 less sensitive to scattered light. This has now been corrected and in the DT campaign  
100 the two fibres should be equally sensitive.
- 101 • The  $d(p/s)/dT_e$  value was obtained by a linear fit to the p/s ratio versus  $T_e$  for a given  
102 pulse number. In the DD measurements a significant offset was observed at the origin.  
103 This offset implied a phenomenon such as stray laser light was causing some  
104 measurement in the ‘p’ channel even at very low  $T_e$ . There is a concern that the  
105 unknown source of this offset could in some way lead to a systematic error in the  
106 measurement of the ‘p’ signal. New polychromators have been used for the DT

---

107 measurements that are significantly more resilient to stray laser light, both because the  
108 filters have stronger optical blocking of the laser line but also because a special  
109 transmissive filter was installed as the first cascade in the polychromator. This  
110 transmissive filter should transmit (and therefore remove) at least 95% of 1064nm  
111 light, so if the offset in the linear fit to the p/s ratio is produced by stray laser light it  
112 should be significantly reduced.

- 113 • The measurements during DD were taken from a single channel polychromator with a  
114 laser line notch filter in front of it. The rationale for this was that in order to improve  
115 the signal to noise ratio the full scattered spectrum could be measured on a single  
116 detector, thereby reducing detector noise. For the measurements during DT we elected  
117 to use a more conventional polychromator design with multiple spectral channels, so  
118 the  $d(p/s)/dT_e$  could be independently calculated for each spectral channel. The  
119 rationale for this is that while it would add some extra random noise to the  
120 measurements, in the form of additional detector noise for each APD utilized, it would  
121 reduce potential systematic error by providing independent measurements.  
122

123 The spectral responsivity of the installed polychromator on JET is shown in Figure 2 with  
124 an overlaid modelled 6keV spectrum at  $\theta=\pi/2$ . A 3-channel polychromator was installed  
125 which should be responsive to temperatures in the  $1\text{keV} < T_e < 10\text{keV}$  range.

### 126 3. Overview of Dataset

127 JET pulses during the DT campaign as indicated in Table 1 form the dataset used to  
128 analyse  $d(p/s)/dT_e$ . These pulses were filtered to remove low temperature pulses as obtaining  
129 good signal to noise ratio for the higher JET pulses with high  $T_e$  is the limiting factor. The  
130 condition for inclusion was at least one second at  $T_e > 4\text{keV}$  was observed, this corresponds to 20  
131 data points as the HRTS laser operates at 20Hz. Applying this filtering 323 JET pulses were  
132 selected for the dataset. In all cases the  $T_e$  is determined from the HRTS measurement point  
133 adjacent to the polarimetric measurements.

134 Figure 3a shows the median  $T_e$  observed during the phase of selected shots where the  $T_e$  is  
135  $> 4\text{keV}$  effectively corresponding to the temperature during the ‘hot’ phase of the pulse. Figure  
136 3b shows the duration of time where these pulses were above 4keV.

137 Once a JET pulse was selected for the dataset, the full duration of that pulse is used  
138 including the low temperature part of the pulse before the heating phase. Since these low  
139 temperature parts of the pulse are significantly longer than the heating phase there are a lot of  
140 low temperature points in the dataset. Sixteen sequential 0.5keV temperature ‘bins’ are defined  
141 from 1keV to 9keV. Each HRTS measurement timeslice is assigned a temperature bin, based on  
142 the measured HRTS temperature at the most high field side point which is adjacent to the image  
143 of fibres with the dedicated ‘p’, ‘s’ and 45 degree polarisers. The number of HRTS timeslices in  
144 each bin is shown in figure 4, as can be seen there are  $> 10,000$  timeslices in the 1-1.5keV bin,  
145  $\sim 500$  timeslices in the 8.5-9keV bin. The number of timeslices in these bins is one of the  
146 fundamental limits on our ability to accurately measure the ‘p/s ratio’ and hence  $d(p/s)/dT_e$ .  
147



---

#### 4. Polarimetric Measurements

Once each timeslice is assigned an appropriate  $T_e$  bin, as described previously, the signal time traces are then accumulated for that bin and then divided by the number of observations in that bin. The time traces for six of the bins are shown in figure 5 to illustrate the data obtained. There are three scattered signals timings corresponding to three delay lines for each time trace as summarised in table 2. The set-up used is such that there are 6 optical fibres combined into a single polychromator, each pulse corresponds to two fibres which have identical delay lines and are adjacent in the plasma. The first pulse, at approximately 80ns has scattered light from a single 's' fibre as well as scattered light from a polariser oriented at 45 degrees so  $0.5 \times (s + p)$ . The second pulse, at approximately 210ns, is connected to two fibres measuring 'p' polarised light. The third pulse, at approximately 380ns is similar to the first pulse measuring the addition of an 's' and 45 degree fibre. The time integral of the three pulses are calculated and the determined ratio of 'p/s' used is pulse 2 / (pulse 1 + pulse 3) which corresponds to  $2 \times p / (3 \times s + p)$  which approximates to  $2/3 \times p/s$ . Details on the design of the HRTS system and fibre delay lines are given in (Pasqualotto 2004 et al).

Figure 5 also illustrates the magnitude of the scattered signals obtained in comparison to the noise fluctuations seen outside of the time windows of interest. At low  $T_e$ , where averaging is performed over many timeslices, the fluctuations are much lower compared to fluctuations observed at high  $T_e$ . These time traces indicate an increasing 'p' scattered signal with increasing  $T_e$ . There is a tendency for low  $T_e$  to be correlated with low  $n_e$  as the low  $T_e$  data are not obtained during the heating phases of JET pulses, hence a comparison of the 'p' and  $1\% \times 's'$  pulses also shown in the figure is required.

For each JET pulse, HRTS diagnostic data acquisition operates for 259 segments, approximately 13 seconds, before the plasma when the laser is firing into the vessel. Measurements taken during this time period are used for straylight subtraction. One of the motivations for measurement during the DT campaign was to remove straylight using a high laser line rejection polychromator, as it was assumed the offset observed in DD originated from transmission by the optical filters of light at 1064nm. The measurements during these 259 segments have subsequently shown that there is very low measureable straylight signal in spectral channel 2, but there is a measurable straylight signal in spectral channel 1 which is approximately 3.4% of the average 's' light observed. For this data set, the averaged time trace obtained during this 259 segment straylight period has in all cases been subtracted from subsequent measurements obtained during plasma. This subtraction was performed on a JET pulse to pulse basis. Initially, no subtraction of straylight was performed and the 'p/s' ratio obtained from channel 1 was found not to be linear with increasing  $T_e$  as the measurement was polluted by this straylight which was much larger than the level of 'p' signal expected. It was found that the subtraction of the straylight had to be performed on a JET pulse to pulse basis in order to obtain a meaningful measurement. This indicates that the straylight level is in fact varying over the plasma pulses observed. It is not clear if the straylight observed in spectral channel 1 is due to transmission at the laser wavelength, or some other in-band source of light related to the laser pulse. In any case, there is much lower straylight observed in spectral channel 2  $\sim 0.46\%$  so the data obtained in this channel is not compromised by this.

191 A comparison of the signal integrals from the ‘p’ and ‘s’ polarisations are shown in figure  
192 6a for spectral channel 1 (the 1017/45nm filter). Up to 2keV the ‘p’ signal approximately equals  
193 the 1% of the ‘s’ signal integral. At higher  $T_e$ , the ‘s’ signal is relatively flat with  $T_e$ , probably a  
194 combination of increasing signal due to higher electron density and decreasing signal due to  $T_e$   
195 shifting the scattered spectrum out of this wavelength band. At these higher  $T_e$ , the ‘p’ signal  
196 increases faster than the ‘s’ signal. A linear fit to the ‘p/s’ ratio is shown in figure 6b. The slope  
197 of the linear fit corresponds well with theoretical predictions of 0.191%/keV. Uncertainties were  
198 derived for the p/s values, these uncertainties are based on the scatter in the signal traces where  
199 there are no scattered pulses and the expected contribution of this to a signal integral.

200 A similar comparison is shown in figure 6c for spectral channel 2. The measurements in  
201 this channel show increasing ‘p’ signal levels above and beyond the ‘s’ signals with increasing  
202  $T_e$ . The linear fit to the ratio shown in figure 6d again shows good agreement on the slope with  
203 theoretical predictions and some offset at  $T_e=0$ . The quality of data for channel 2 appears better  
204 than that in channel 1, this might be the case because a) at the temperatures of interest there is  
205 more signal in spectral channel 2 improving data quality and b) there is much lower straylight in  
206 spectral channel 2 (~0.46% of ‘s’ signal) compared with spectral channel 1 (~3.4% of ‘s’ signal)  
207 which may impact on measurements. Results from channel 3 are also shown in figure 6e and 6f  
208 for completeness but are not considered as the scattered signal levels are much lower than in  
209 channels 1 and 2 and not high enough to provide good ‘p’ signal measurements.

210 The theoretical estimate of a linear variation of 0.191%  $d(p/s)/dT_e$  is a very good  
211 approximation. If we numerically determine the derivative, values of ~0.187/keV% and  
212 ~0.194/keV% are obtained at 1keV and 8keV respectively. To represent this non-linearity an  
213 error bar has been assigned to the theoretical prediction in table 3.

214 In order to estimate the uncertainty on the determined  $d(p/s)/dT_e$ , a Monte Carlo approach  
215 was taken varying which JET pulses were accumulated and examining the resulting  $d(p/s)/dT_e$   
216 parameter and offsets. Monte Carlo runs were constructed by randomly including individual  
217 JET pulses with a 50% probability from the full 323 pulses in the dataset. Hence each individual  
218 Monte Carlo run had ~160 pulses. The results of 100 such Monte Carlo runs are shown in figure  
219 7 where the resulting  $d(p/s)/dT_e$  are shown for spectral channels 1 and 2. To illustrate the  
220 variation in results, the value of  $d(p/s)/dT_e$  are plotted in ascending order for each channel. This  
221 shows that the  $d(p/s)/dT_e$  values determined in spectral channel 1 and spectral 2 are both under  
222 the theoretical estimate. For the spectral channel 1 the mean value determined is within 1-sigma  
223 of the theoretical range. For the spectral channel 2 dataset the mean value determined is close to  
224 2-sigma away from the theoretical estimate.

## 225 5. Conclusions

226 The aim of this work was to verify the technique of polarimetric Thomson scattering for  
227 use on ITER. Thomson scattering is inherently a difficult measurement to make as you need to  
228 obtain a rejection of stray laser light of approximately  $n_e \times \sigma_{Te} \sim 10^{-10}$  using optical rejection of  
229 filters and geometry which is challenging. Polarimetric Thomson scattering is even more  
230 challenging as it is typically a factor  $10^2$  below ‘s’ Thomson scattered light and it is required to  
231 distinguish the ‘p’ light from the ‘s’ light. The key measurements obtained in this work are  
232 summarised in table 3. The main conclusion of this work is then that the  $d(p/s)/dT_e$  obtained is  
233 close to theoretical predictions as measured independently by two spectral bands of a

---

234 polychromator. This gives support to application of this technique on ITER. The discrepancy  
235 between the theoretical predictions and experimental measurements are larger than the error  
236 bars obtained by including random pulses. This we cannot fully explain, but attribute to the very  
237 small signal levels we are measuring and sensitivities to systematic effects.

238 That similar results are obtained in spectral channels 1 and 2 despite some  $\sim 3.37\%$   
239 straylight being observed in spectral channel 1 indicates that pollution due to straylight observed  
240 in previous experiments did not significantly influence those results.

241 Both spectral channel 1 and 2 see a non-negligible offset signal in the ‘p’ channel that we  
242 interpret as ‘bleed through’. At this low level, a number of origins for this offset are possible, it  
243 could be due to physical accuracy of polariser installation, laser beam polarisation or extinction  
244 ratio of the polariser. Alternatively it could be some combination of these phenomena.

245 The measurements taken on JET show the variation of p/s with  $T_e$  over a few hundred JET  
246 pulses and with  $\sim 19,000$  samples over 4keV. The goal of this technique as applied to ITER is to  
247 do the opposite and infer  $T_e$  from p/s. JET has one advantage over ITER in measurement of  
248 polarimetric Thomson scattering, it is at a favourable scattering angle. This favourable  
249 scattering provides  $3\times$  as many photons. ITER has two significant advantages over JET, the  
250 core plasma Thomson scattering system will operate at 100Hz and it can install measurement  
251 samples of polarimetric light across the full laser chord giving it up to  $\sim 70$  spatial samples  
252 compared to a single spatial sample on JET. Hypothetically then for a 20keV peaking profile on  
253 ITER, a polarimetric measurement with equivalent quality to the full  $\sim 19,000$  samples from this  
254 JET dataset could be obtained in tens of seconds of an ITER discharge by averaging over a  
255 number of spatial points from the Core Plasma Thomson scattering diagnostic.

## 256 Acknowledgments

257 The authors would like to acknowledge all the contributors that made possible the high  
258 temperature pulses on JET used in this publication. That includes all those control room staff  
259 who were involved in the running of the experiments such as diagnostic co-ordinators and  
260 session leaders. It also includes all those involved in the design of the pulses, the JET DT Task  
261 force leaders and in particular the scientific co-ordinators: D. Frigione, L. Garzotti, F. Rimini,  
262 D. Van Ester, C. Challis, J. Hobirk, A. Kappatou, E. Lerche, D. Keeling, R. Dumont, M.  
263 Maslov, P. A. Schneider, Y. Kazakov, M. Nocente, S. Brezinsek, C. Giroud, P. Mantica, S.  
264 Sharapov, R. Dumont, M. Fitzgerald, D. King, A. Kirschner, M. Mantsinen and P. Jacquet.

265 This work has been carried out within the framework of the EUROfusion Consortium, funded  
266 by the European Union via the Euratom Research and Training Programme (Grant Agreement  
267 No 101052200 — EUROfusion). Views and opinions expressed are however those of the  
268 authors only and do not necessarily reflect those of the European Union or the European  
269 Commission. Neither the European Union nor the European Commission can be held  
270 responsible for them. This work has also been funded by EPSRC under grant EP/W006839/1.

## 271 References

- 272 [1] (Giudicotti et al, 2018) L. Giudicotti et al 2018 Nucl. Fusion 58 044003  
273 <https://doi.org/10.1088/1741-4326/aab3fd>  
274  
275 [2] (Scannell R. et al 2017) <https://doi.org/10.1088/1748-0221/12/11/C11010>

276  
277 [3] (Orsitto F et al 1999) Review of Scientific Instruments 70, 798 (1999);  
278 <https://doi.org/10.1063/1.1149414>

279  
280 [4] (Segre S.E. et al 2000) <https://aip.scitation.org/doi/10.1063/1.874110>  
281

282 [5] (Parke E. et al 2014) <https://iopscience.iop.org/article/10.1088/1748-0221/9/02/C02030>

283  
284 [6] (Mirnov V.V. et al ) <https://aip.scitation.org/doi/10.1063/1.4948488>

285  
286 [7] (Pasqualotto et al 2004) Review of Scientific Instruments 75, 3891 (2004);  
287 <https://doi.org/10.1063/1.1787922>

288  
289  
290  
291  
292  
293

<i>Condition for Inclusion</i>	1s > 4keV
<i>First JET Pulse</i>	99147
<i>Last JET Pulse</i>	99982
<i>No. of JET Pulses used</i>	323
<i>No. of HRTS segments &gt;4keV</i>	19051

294 Table 1 - Key parameters of the JET DT campaign database used for analysis.

295

<i>Scattered Signal/ Delay line</i>	<b>Fibre 1 polariser</b>	<b>Fibre 2 polariser</b>
<i>#1: ~80ns</i>	S	45 degree
<i>#2: ~220ns</i>	P	P
<i>#3: ~380ns</i>	S	45 degree

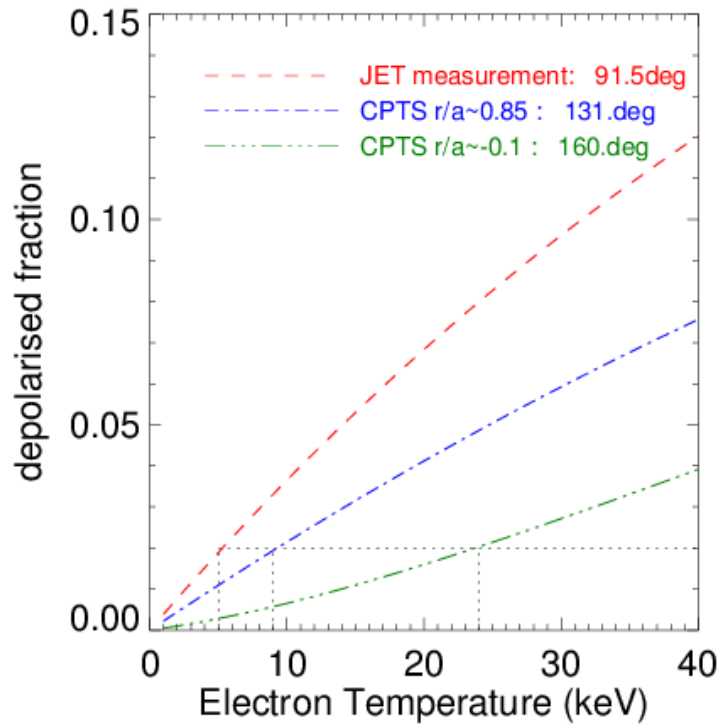
296 Table 2 - Fibres used in polarimetric spectrometer with corresponding polarizer orientations and  
297 scattered signal timings.

298

299

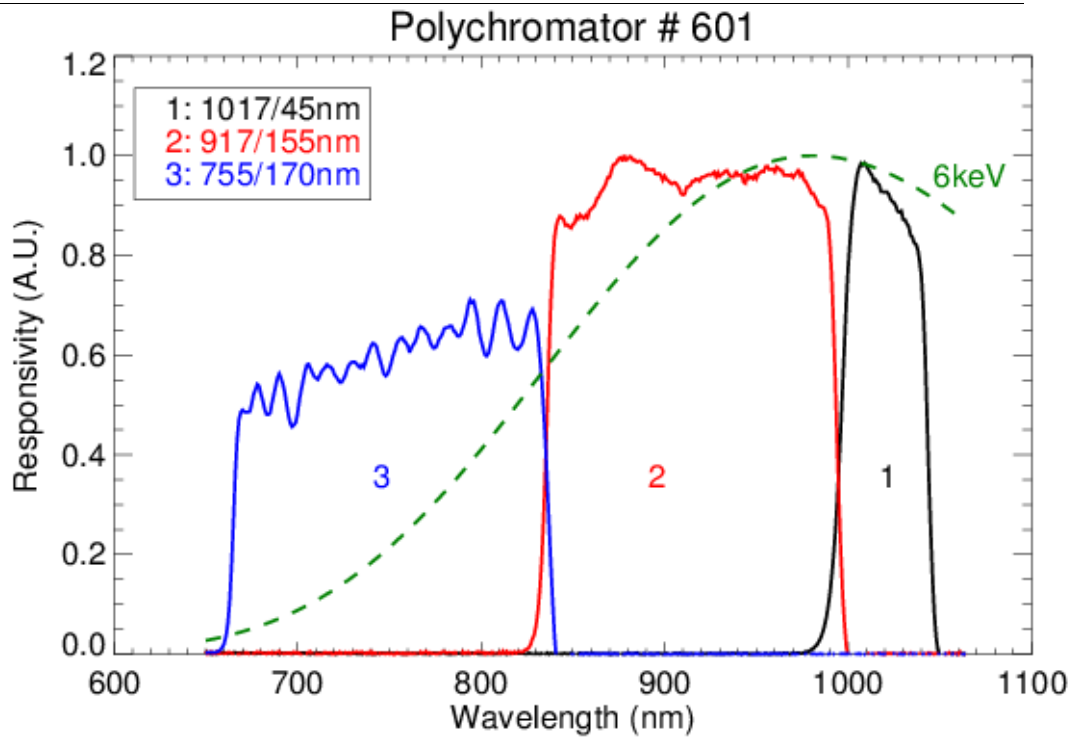
	<b>Straylight light before plasma</b>	<b>Bleed through offset of linear fit</b>	<b>d(p/s)/dT<sub>e</sub> (%/keV)</b>
Theoretical Prediction	-	-	0.187-0.194
Channel 1	3.37%	0.796±0.122%	0.178±0.037%
Channel 2	0.46%	0.638±0.067%	0.158±0.017%

300 Table 3 – Comparison of theoretical and experimentally observed increase in p/s ratio with electron  
301 temperature for various spectral channels. Uncertainty estimates are obtained from Monte Carlo analysis.  
302 Spectral Channel 3 is excluded due to large uncertainty.



303  
304  
305  
306  
307  
308  
309

Figure 1. Fraction of light depolarized as a function of electron temperature, for the JET measurements and for the two extreme scattering angles of the ITER CPTS diagnostic.

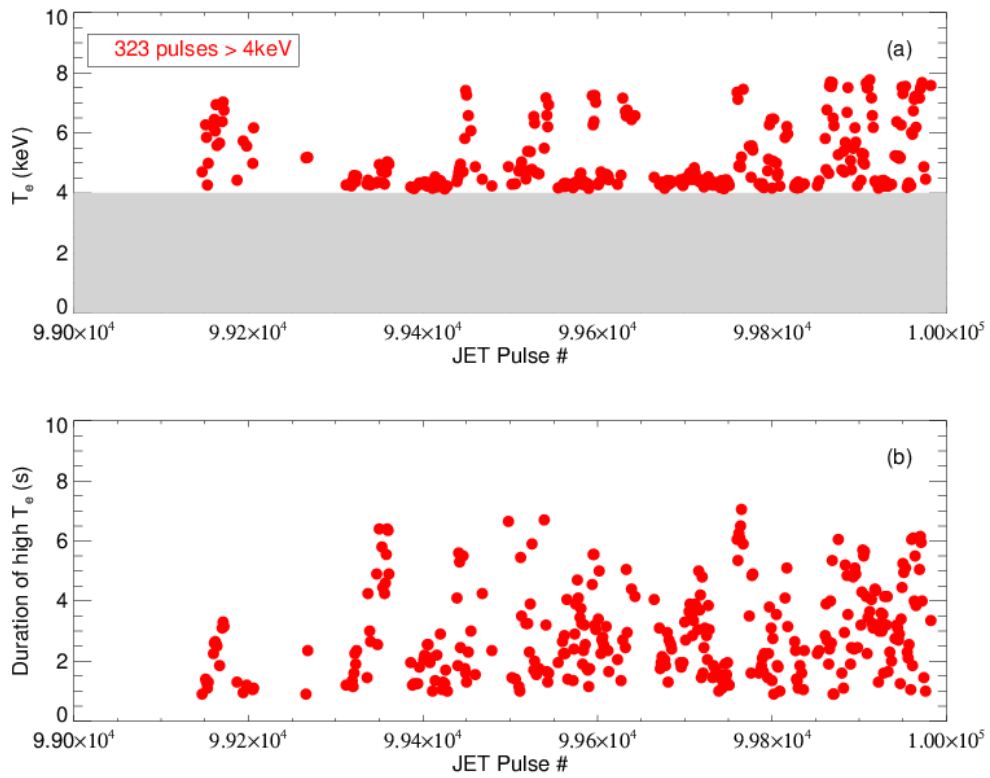


310

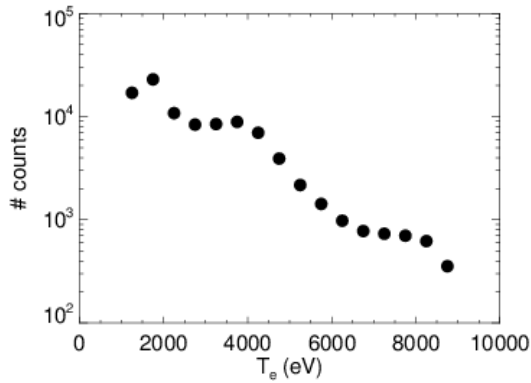
311

312 Figure 2. Spectral responsivity of the polychromator installed to detect 'p' polarized light.

313 Also shown is the spectral intensity of the expected light at 6keV.

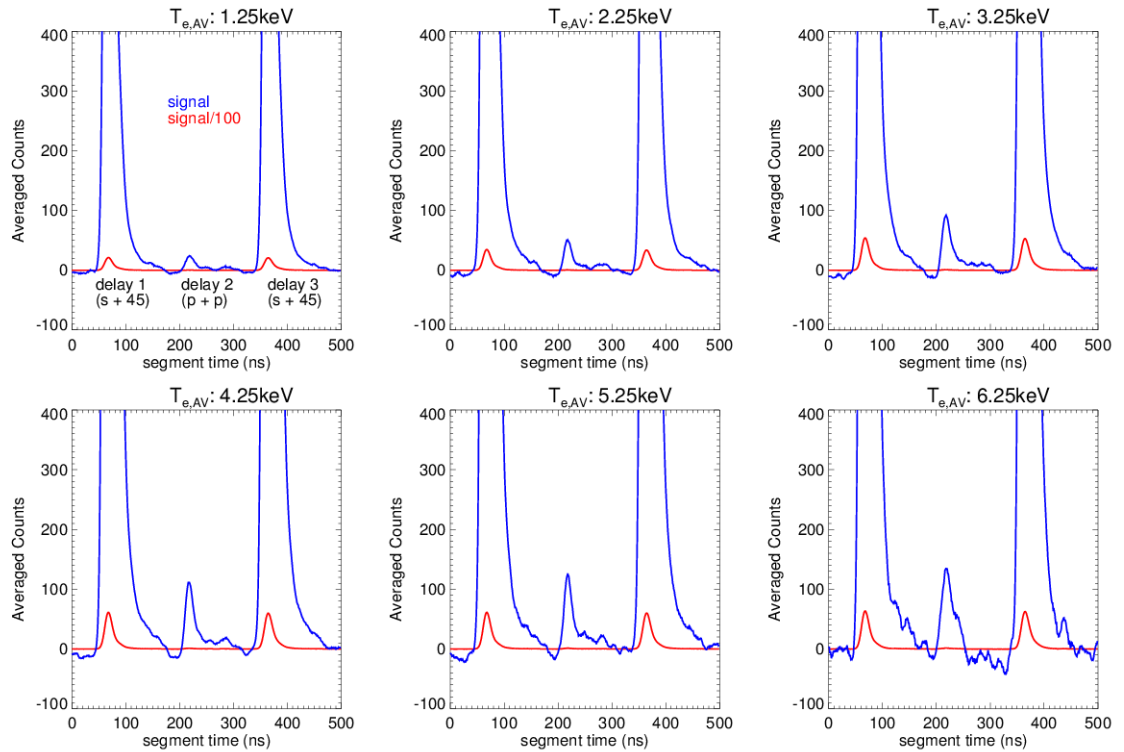


314  
 315 Figure 3. (a) Median  $T_e$  observed during the hot ( $>4\text{keV}$ ) phase of JET pulses and (b)  
 316 duration of the  $>4\text{keV}$  period of these pulses.  
 317



318  
 319 Figure 4. Number of counts observed in 500eV temperature bins used to construct the  
 320 dataset.  
 321  
 322

323  
324

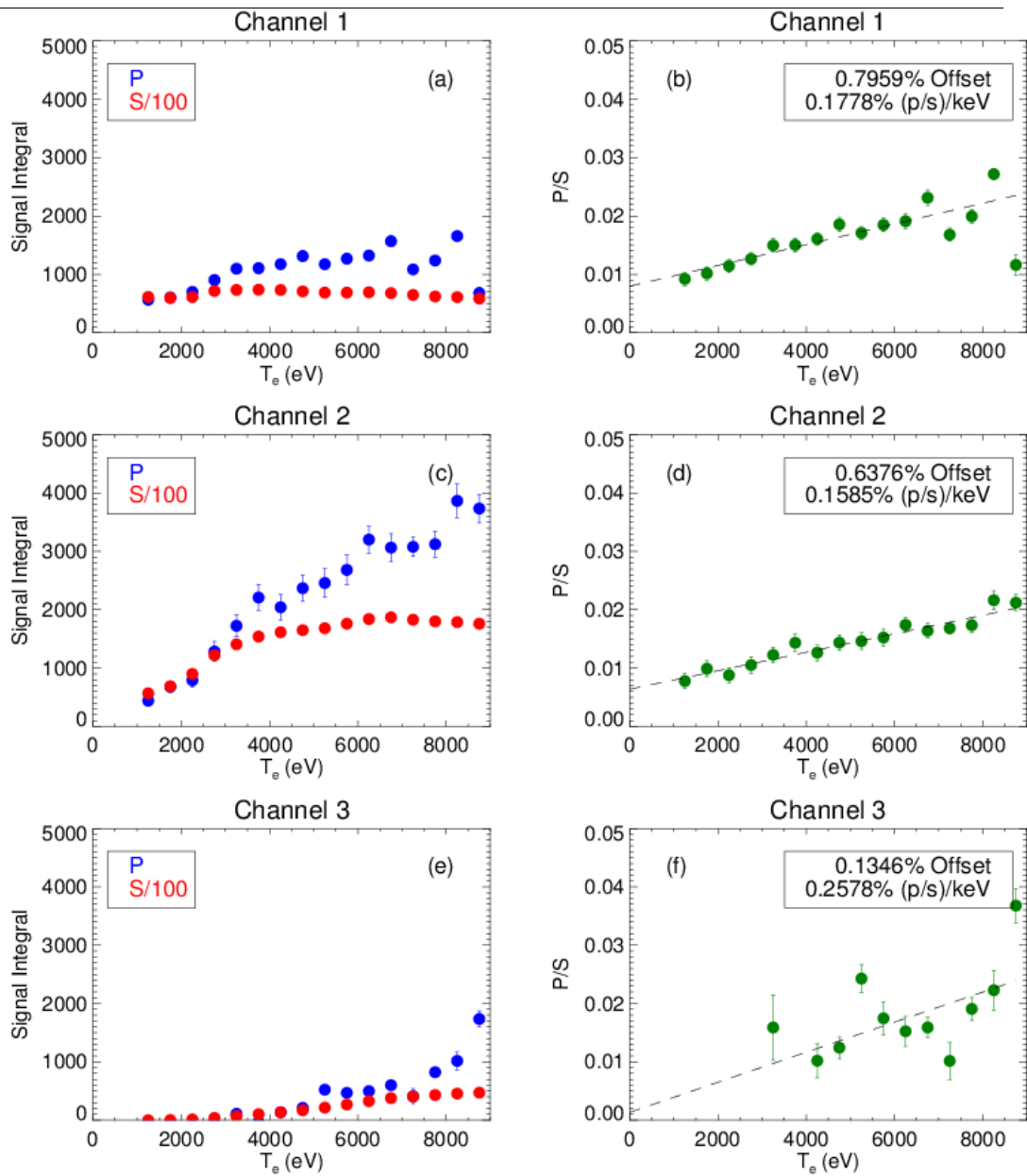


325

326 Figure 5 – Time traces of scattered signals observed in spectral channel 2 for six temperature bins  
327 accumulated over the full dataset. Each time trace has three pulses with different optical delays. Each  
328 pulse comes from two fibres with the same optical delay line. The first and third pulses, at ~80ns and  
329 ~380ns respectively, each come from one fibre with an ‘s’ polarizer and one fibre with a 45 degree  
330 polarizer. The second pulse at ~210ns comes from two fibres with ‘p’ polarisers. The fibres are located in  
331 adjacent spatial channels in the plasma. As well as the averaged scattered signal trace a second trace  
332 illustrating 1% of the scattered signal trace is overlaid.

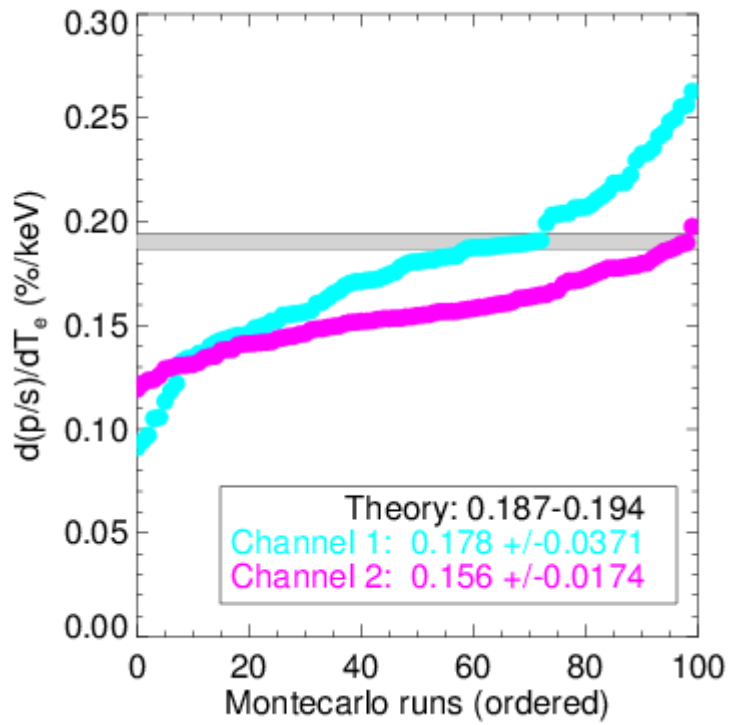
333  
334  
335  
336  
337  
338





339  
 340  
 341  
 342  
 343  
 344  
 345  
 346

Figure 6 – For spectral channels 1, 2 and 3, the change in ‘p’ and ‘s’ signal integrals with  $T_e$  are shown as well as the increase in the ‘p/s’ ratio with  $T_e$ . For the plots showing the ratio, a linear fit and best fit parameters of that linear fit are provided in the legend. These data here is determined by accumulating the full dataset in contrast with the values in figure 7 obtained from subsets of this full dataset.



347  
 348 Figure 7 – Results of slope  $d(p/s)/dT_e$  from Monte Carlo runs, where each JET discharge is  
 349 randomly included or excluded from the dataset in each run. The determined slopes for each run  
 350 have been arranged in ascending order for each spectral bin for illustrative purposes and  
 351 comparison with the theoretical values.